

See discussions, stats, and author profiles for this publication at: <https://www.researchgate.net/publication/231667678>

Significant Reduction in Adsorption Energy of CO on Platinum Clusters on Graphite

ARTICLE *in* JOURNAL OF PHYSICAL CHEMISTRY LETTERS · DECEMBER 2009

Impact Factor: 7.46 · DOI: 10.1021/jz900158y

CITATIONS

25

READS

31

9 AUTHORS, INCLUDING:



Yoshiyuki Suda

Toyohashi University of Technology

105 PUBLICATIONS 500 CITATIONS

SEE PROFILE

Significant Reduction in Adsorption Energy of CO on Platinum Clusters on Graphite

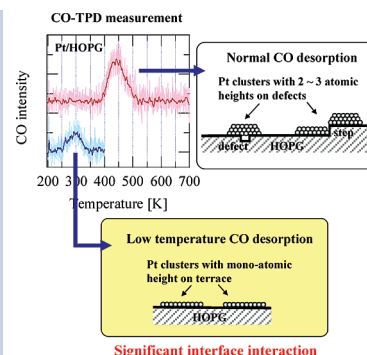
Junepyo Oh,[†] Takahiro Kondo,[†] Daigo Hatake,[†] Yosuke Iwasaki,[†] Yujiro Honma,[†] Yoshiyuki Suda,[‡] Daiichiro Sekiba,[§] Hiroshi Kudo,[§] and Junji Nakamura^{*,†}

[†]Graduate School of Pure and Applied Science, University of Tsukuba, 1-1-1 Tennoudai, Tsukuba, Ibaraki 305-8573, Japan,

[‡]Department of Electrical and Electronic Engineering, Toyohashi University of Technology, 1-1 Hibarigaoka, Tempaku, Toyohashi, Aichi 441-8580, Japan, and [§]Tandem Accelerator Complex, Research Facility Center for Science and Technology, and Institute of Applied Physics, University of Tsukuba, 1-1-1 Tennoudai, Tsukuba, Ibaraki 305-8573, Japan

ABSTRACT We have studied desorption of CO on a Pt-deposited highly oriented pyrolytic graphite (HOPG) surface by temperature programmed desorption of CO (CO-TPD), scanning tunneling microscope (STM), and He atom scattering (HAS). A desorption peak of CO at a significantly lower temperature of ~ 270 K with a heating rate of 0.5 K/s is observed for Pt clusters on a flat terrace of HOPG. STM results indicate that the height of Pt clusters on the terraces of the HOPG surface is monatomic. It is concluded that the significant reduction in CO adsorption energy is due to a modified electronic structure as a result of the interface interaction between Pt clusters and the HOPG surface.

SECTION Surfaces, Interfaces, Catalysis



Reduction of Pt usage or promotion of Pt catalytic activity is very important for commercializing fuel cells.^{1,2} The significant support effect of carbon on the catalytic activity of Pt has been reported.^{3–8} For example, thick multiwalled carbon nanotubes are superior to carbon black as a support material for electrocatalysts. The Pt usage in fuel cells is thus expected to be reduced by taking advantage of the carbon support effect. Surface science studies using Pt/graphite model catalysts have been carried out to explore the detailed mechanism of the support effect. It has been found that Pt monolayer clusters with 2–3 nm width on a highly oriented pyrolytic graphite (HOPG) surface show promoted catalytic activity for the $\text{H}_2\text{--D}_2$ exchange reaction.⁹ This indicates significant interface interaction between Pt and graphite, and the promotion is attributed to a shift in the d-band center of Pt away from the Fermi level. In the present work, the adsorption of CO on Pt/HOPG has been examined by temperature programmed desorption (TPD) and helium atom scattering (HAS).

The existence of Pt atoms on HOPG was confirmed by ex situ Rutherford backscattering spectroscopy (RBS), ex situ scanning electron microscopy (SEM), and scanning tunneling microscopy (STM). The results of RBS, SEM, and STM measurements for the pristine HOPG and the Pt-deposited HOPG are shown in Figure 1. On the basis of the RBS signal, the Pt coverage was estimated as $\theta_{\text{Pt}} = 0.18$, where $\theta_{\text{Pt}} = 1$ is defined as the number of carbon atoms per unit surface area. The RBS spectrum indicated that only carbon and platinum are present in Pt/HOPG, i.e., no impurities and/or different metals are present. In the SEM images of Pt/HOPG in Figure 1b, black spots and bright spots are observed on a terrace of HOPG. It is also confirmed by STM images of

Figure 1 (c) that Pt clusters with the size of 1–2 nm are deposited on the terrace of HOPG.

Figure 2a shows the CO-TPD results at Pt coverage (θ_{Pt}) 0, 0.12, 0.18, and 0.24. Two main desorption peaks of CO appear at ca. 270 and 440 K, and no adsorption of CO was observed for $\theta_{\text{Pt}} = 0$. The desorption peak at 440 K is similar to those observed for Pt single crystal surfaces: 498 K for Pt(111) ($\beta = 50 \text{ K s}^{-1}$), 523 K for Pt(110) ($\beta = 4 \text{ K s}^{-1}$), 552 K for Pt(100) ($\beta = 50 \text{ K s}^{-1}$), 428 and 554 K for Pt(321) ($\beta = 10 \text{ K s}^{-1}$).^{10–13} However, the CO desorption peak at 270 K has not been reported for any type of Pt single crystal surface. The CO adsorption energies derived from the peak at 270 K and the peak at 440 K are roughly estimated as 73 and 121 kJ mol^{-1} from Redhead's equation, respectively.¹⁴ The CO adsorption energy of 73 kJ mol^{-1} is comparable with those for Cu (82 kJ mol^{-1}) and Au (74 kJ mol^{-1}).^{15,16} Thus Pt clusters with special chemical properties were formed on HOPG. The intensity of the CO desorption peak at 270 K decreased with increasing Pt coverage on HOPG, and the CO desorption peak at 440 K became dominant at $\theta_{\text{Pt}} = 0.24$ (Figure 2a).

Figure 2b shows the result of in situ HAS at $\theta_{\text{Pt}} = 0$ and 0.12, in which the surface temperature dependence of the specularly reflected intensity of He was recorded concurrently with CO-TPD. It is widely known that the specularly reflected intensity of He is that from the flat terraces of the surface. The scattering intensity from defects (such as vacancy, step, kink, adatoms, and a specifically charge modulated site) is not

Received Date: October 18, 2009

Accepted Date: December 8, 2009

Published on Web Date: December 22, 2009

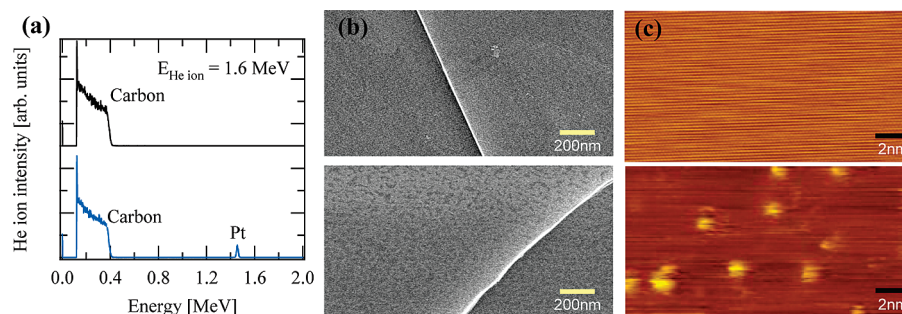


Figure 1. (a) RBS data of the pristine HOPG (black curve) and Pt as-deposited HOPG (blue curve). The 1.6 MeV He ion (~ 2.5 nA) was used, and the backscattered ions were detected by a solid state detector (SSD) at the angle of 153° with respect to the beam incident direction; SEM and STM images are shown in panels b and c, respectively. Top row shows the images of the pristine HOPG, and bottom row shows the images of Pt as-deposited HOPG.

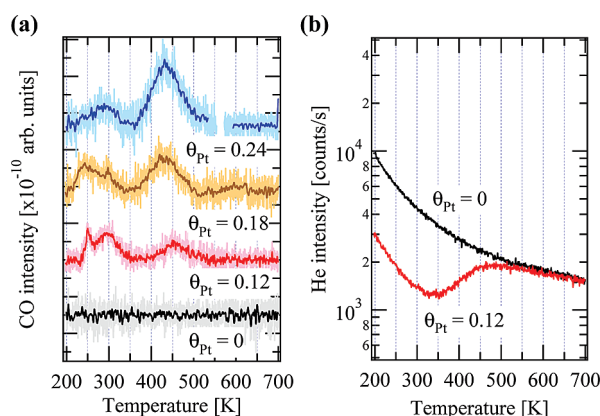


Figure 2. (a) TPD data of CO adsorbed on as-deposited Pt/HOPG with varying Pt coverage; (b) in situ HAS data for $\theta_{Pt} = 0.12$ during the CO-TPD experiment. The heating rate was 0.5 K s^{-1} . 1 % CO/N₂ was dosed for 5 min to HOPG with surface temperature $T_s = 250 \text{ K}$.

included due to the diffuse scattering of He at such sites. Note that a terrace in the vicinity of a defect does not contribute to the specularly reflected intensity of He because of the large scattering cross-section (typically about 100 \AA^2).^{17,18} The intensity at $T_s = 200 \text{ K}$ for $\theta_{Pt} = 0.12$ is smaller than that for $\theta_{Pt} = 0$, indicating that the area of the flat terrace site decreases by the Pt deposition, i.e., some of the Pt atoms should be located on the flat terrace site of HOPG. The He intensity (Figure 2b) for the pristine HOPG surface ($\theta_{Pt} = 0$) decreases monotonically with increasing surface temperature due to the Debye–Waller effect.^{19,20} In the same manner, the intensity for $\theta_{Pt} = 0.12$ decreases with increasing surface temperature up to 350 K. However, the specularly reflected intensity of He increases from 350 to 500 K. This increase in He intensity suggests that the flat terrace area on the Pt/HOPG surface increased by diffusion of the Pt atoms from the terrace sites to defect sites or by a morphological change of the Pt clusters. Above 500 K, the intensity became almost the same as that of the pristine HOPG surface. This indicates significant changes in Pt clusters on the flat terraces. It was confirmed by RBS and SEM results (see Supporting Information) that desorption of Pt atoms and diffusion of Pt atoms into the graphite did not occur.

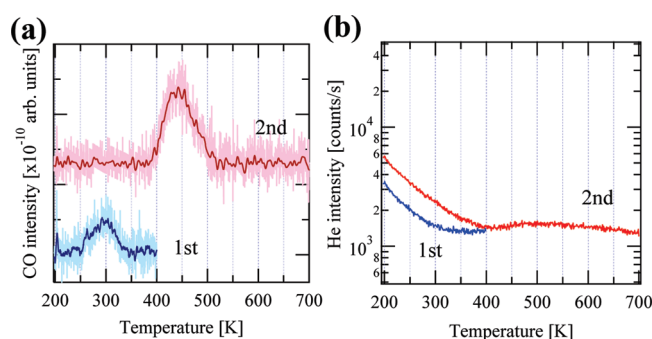


Figure 3. (a) CO-TPD measurement and (b) in situ HAS data of the as-deposited Pt/HOPG ($\theta_{Pt} = 0.18$). Pt deposition and CO dosing were performed at HOPG surface temperature $T_s = 250 \text{ K}$.

To examine the behavior of Pt clusters between 300 and 400 K, simultaneous CO-TPD and in situ HAS were repeated after the measurements up to 400 K, as shown in Figure 3a,b. CO was dosed again at 200 K after the first measurements. The CO desorption peak of 270 K was observed in the first TPD experiment up to 400 K, but that peak vanished in the second run (Figure 3a), and only the desorption peak at 440 K was observed. The He intensity did not decrease between 300 and 400 K in the first experiment, but a decrease was observed in that temperature range in the second run (Figure 3b), indicating that the area of the flat terrace increased during heating at 300–400 K in the first run. The integrated area of the CO peak at 440 K in the second run is increased compared to that of the normal TPD run at the same Pt coverage. This is also due to the condensation (and/or morphological change) by heating of the special Pt clusters that gave rise to the 270 K peak. It is concluded that the special Pt clusters that gave rise to the 270 K peak were located on the flat terraces of HOPG.

In order to observe the morphology of the Pt clusters on the flat terraces of HOPG, STM measurements were carried out for Pt/HOPG with and without heating at 400 K. In Figure 4a,c, the bright spots in the image correspond to the Pt clusters. In the Pt as-deposited HOPG, the Pt clusters on the terrace of HOPG were found to have raft-like structure with monatomic height and 1–3 nm diameters, as shown by the height–diameter distribution of Figure 4b. On the other hand, for the Pt/HOPG after heating to 400 K, Pt clusters of more than

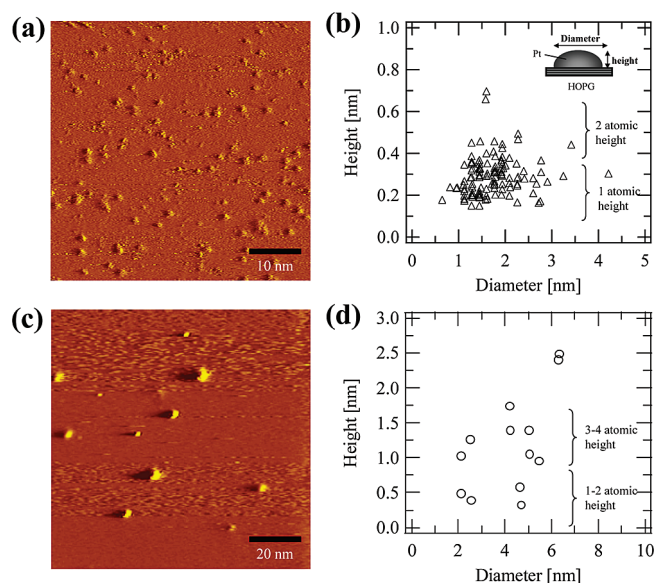


Figure 4. STM current image of (a) Pt as-deposited HOPG (scan range $50 \times 50 \text{ nm}^2$, tunneling current $I_t = 150 \text{ pA}$, and sample bias $V_s = 0.30 \text{ V}$) and (c) Pt/HOPG after heating to 400 K (scan range $100 \times 100 \text{ nm}^2$, tunneling current $I_t = 156 \text{ pA}$, and sample bias $V_s = 0.10 \text{ V}$). (b,d) Distributions of cluster heights obtained from the topographical STM image as a function of the corresponding cluster diameter.

3 atomic heights and 2–6 nm diameters were mainly observed, as shown in Figure 4d. The STM results indicate that the heating at 400 K lead to the condensation and the morphological change of Pt clusters. This explains well the change of He intensity during the first CO-TPD measurement of Figure 3b. Similar height-diameter distribution of Pt clusters on HOPG without the heating has also been reported in the literature.^{9,21} It is thus considered that the Pt clusters with a CO desorption peak of 270 K can be ascribed to the flat Pt clusters with monatomic height located on the terraces of HOPG.

Here, we discuss the mechanism of the weakening of Pt–CO binding. The electronic state of such a flat Pt cluster on HOPG should be different from that of bulk Pt, since the Pt–Pt distance is shorter than that in bulk Pt by 13%.^{8,21} Also, it has been observed that the Pt atom is located on the β -carbon of the HOPG surface. The reduction in the Pt–Pt distance results in a shift of the d-band center of Pt away from the Fermi level. The lower shift of the d-band center leads to lower adsorption energy of CO.^{22,23} On the other hand, when the Pt coverage is increased or the Pt cluster is condensed at a step edge and/or defect, the height of the Pt cluster becomes taller, and the interface interaction (lower shift of the d-band center) disappears. The adsorption energy of Pt–CO then becomes the same as that of single crystal Pt.

In summary, we found that the adsorption energy of CO on the Pt clusters with monatomic height on the terraces of an HOPG surface is significantly small as 73 kJ/mol. On the basis of CO-TPD, STM, and HAS results, we conclude that the significant reduction in the CO adsorption energy is due to a modified electronic structure of the Pt clusters, which is different from that of bulk Pt. The formation of the Pt clusters

is ascribed to the interface interaction between Pt clusters and the HOPG surface. The advantage of the interface interaction between metal clusters and the graphitic carbon surface is expected to reduce with the usage of precious metal catalysts or the development of alternate precious catalysts by non-precious metal.

EXPERIMENTAL METHODS

All experiments were performed in an ultrahigh vacuum (UHV) system with base pressure about 3×10^{-10} Torr. A supersonic molecular beam of He or CO was generated by free-jet expansion in the molecular beam source chamber. The beam diameter and cross-section areas on the sample surface at the scattering chamber are 2.5 mm and 4.9 mm^2 , respectively (see ref 24 for details of the apparatus).

The sample surface of HOPG (NT-MDT Co., Russia, 12 mm \times 12 mm \times 1.5 mm, grade ZYA) was cleaved in air by adhesive tape and then put into a UHV scattering chamber. The HOPG sample was mounted on a sample holder, which can be cooled down to 90 K by a cryogenic refrigerator head (Iwatani CryoMini S050) and can be heated by the infrared radiation from a hot tungsten filament placed close to the back side of the HOPG sample. The surface temperature of HOPG was measured by a type-K thermocouple attached on the sample surface by a Ta clamp. Prior to the experiment, the HOPG sample was annealed at 900 K in UHV for 5 min in order to clean the surface.

Pt atoms were deposited onto HOPG by resistively heating a Pt wire (Nilaco Co., $\phi = 0.3 \text{ mm}$, length = 8 cm). The surface temperature of HOPG was maintained at a constant value by a temperature controller during Pt vapor deposition. Characterization of Pt nanoclusters on HOPG was performed using STM (USM-1300S), ex situ RBS technique, and ex situ SEM (Hitachi, S-4800). STM measurements were separately conducted in a different UHV chamber, but the experimental conditions such as Pt deposition time were set to the same as those in the main experimental UHV chamber. CO-TPD and HAS were measured simultaneously for Pt/HOPG samples with various Pt coverage (θ_{Pt}). A molecular beam of CO (1 % in N_2 , 5.24×10^{14} molecules ($\text{cm}^2 \cdot \text{s}^{-1}$)) was dosed to the sample for 5 min, then CO-TPD was carried out at a 0.5 K s^{-1} heating rate. During heating of the sample surface in the TPD experiment, the morphological change of Pt clusters on the HOPG surface was examined by monitoring the reflection intensity of the He beam.^{17,18}

SUPPORTING INFORMATION AVAILABLE Supporting results (HAS, RBS data, and SEM images) included. This material is available free of charge via the Internet at <http://pubs.acs.org>.

AUTHOR INFORMATION

Corresponding Author:

*To whom correspondence should be addressed. TEL/FAX: +81-29-853-5279. E-mail: nakamura@ims.tsukuba.ac.jp.

ACKNOWLEDGMENT This work was supported by NEDO (New Energy and Industrial Technology Organization) under the METI

(The Ministry of Economy, Trade and Industry, Japan). We thank Mr. Ishii for his kind support during RBS measurement at UTTAC at the University of Tsukuba.

REFERENCES

- (1) Bashyam, R.; Zelenay, P. A Class of Non-precious Metal Composite Catalysts for Fuel Cells. *Nature* **2006**, *443*, 63–66.
- (2) Stamenkovic, V. R.; Fowler, B.; Mun, B. S.; Wang, G.; Ross, P. N.; Lucas, C. A.; Markov, N. M. Improved Oxygen Reduction Activity on Pt₃Ni(111) via Increased Surface Site Availability. *Science* **2007**, *315*, 493–497.
- (3) Tang, H.; Chen, J. H.; Hung, Z. P.; Wang, D. Z.; Ren, Z. F.; Nie, L. H.; Kuang, Y. F.; Yao, S. Z. High Dispersion and Electrocatalytic Properties of Platinum on Well-Aligned Carbon Nanotube Arrays. *Carbon* **2004**, *42*, 191–197.
- (4) Liu, Z.; Lin, X.; Lee, J. Y.; Zhang, W.; Han, M.; Gan, L. M. Preparation and Characterization of Platinum-Based Electrocatalysts on Multiwalled Carbon Nanotubes for Proton Exchange Membrane Fuel Cells. *Langmuir* **2002**, *18*, 4054–4060.
- (5) Britto, P. J.; Santhanam, K. S. V.; Angel, R.; Julio, A. A.; Ajayan, P. M. Improved Charge Transfer at Carbon Nanotube Electrodes. *Adv. Mater.* **1999**, *11*, 154–157.
- (6) Yin, S. F.; Xu, B. Q.; Ng, C. F.; Au, C. T. Nano Ru/CNTs: A Highly Active and Stable Catalyst for the Generation of CO_x-Free Hydrogen in Ammonia Decomposition. *Appl. Catal., B* **2004**, *48*, 237–241.
- (7) Yoo, E.; Okada, T.; Akita, T.; Kohyama, M.; Nakamura, J.; Honma, I. Enhanced Electrocatalytic Activity of Pt Subnanoclusters on Graphene Nanosheet Surface. *Nano Lett.* **2009**, *9*, 2255–2259.
- (8) (a) Matsumoto, T.; Komatsu, T.; Arai, K.; Yamazaki, T.; Kijima, M.; Shimizu, H.; Takasawa, Y.; Nakamura, J. Reduction of Pt Usage in Fuel Cell Electrocatalysts with Carbon Nanotube Electrodes. *Chem. Commun.* **2004**, *7*, 840–841. (b) Matsumoto, T.; Komatsu, T.; Nakano, H.; Arai, K.; Nagashima, Y.; Yoo, E.; Yamazaki, T.; Kijima, M.; Shimizu, H.; Takasawa, Y.; Nakamura, J. Efficient Usage of Highly Dispersed Pt on Carbon Nanotubes for Electrode Catalysts of Polymer Electrolyte Fuel Cells. *Catal. Today* **2004**, *90*, 277–281. (c) Yoo, E.; Okada, T.; Kizuka, T.; Nakamura, J. Effect of Various Carbon Substrate Materials on the CO Tolerance of Anode Catalysts in Polymer Electrolyte Fuel Cells. *Electrochemistry* **2007**, *2*, 146–148. (d) Yoo, E.; Okada, T.; Kizuka, T.; Nakamura, J. Effect of Carbon Substrate Materials As a Pt–Ru Catalyst Support on the Performance of Direct Methanol Fuel Cells. *J. Power Sources* **2008**, *180*, 221–226. (e) Oh, J.; Yoo, E.; Ono, C.; Kizuka, T.; Okada, T.; Nakamura, J. Support Effect of Anode Catalysts Using an Organic Metal Complex for Fuel Cells. *J. Power Sources* **2008**, *185*, 886–891.
- (9) Kondo, T.; Izumi, K.; Watahiki, K.; Iwasaki, Y.; Suzuki, T.; Nakamura, J. Promoted Catalytic Activity of a Platinum Monolayer Cluster on Graphite. *J. Phys. Chem. C* **2008**, *112*, 15607–15610.
- (10) Ertl, G.; Neumann, M.; Streit, K. M. Chemisorption of CO on the Pt(111) Surface. *Surf. Sci.* **1977**, *64*, 393–410.
- (11) Hofmann, P.; Bare, S. R.; King, D. A. Surface phase transitions in CO chemisorption on Pt(110). *Surf. Sci.* **1982**, *117*, 245–256.
- (12) McClellan, M. R.; Gland, J. L.; McFeeley, F. R. Carbon Monoxide Adsorption on the Kinked Pt(321) Surface. *Surf. Sci.* **1981**, *112*, 63–77.
- (13) McCabe, R. W.; Schmidt, L. D. Binding States of CO on Single Crystal Planes of Pt. *Surf. Sci.* **1977**, *66*, 101–124.
- (14) Redhead, P. A. Thermal Desorption of Gases. *Vacuum* **1962**, *12*, 203–211.
- (15) Dulaurent, O.; Courtois, X.; Perrichon, V.; Bianchi, D. Heats of Adsorption of CO on a Cu/Al₂O₃ Catalyst Using FTIR Spectroscopy at High Temperatures and under Adsorption Equilibrium Conditions. *J. Phys. Chem. B* **2000**, *104*, 6001–6011.
- (16) Derrouiche, S.; Gravejat, P.; Bianchi, D. Heats of Adsorption of Linear CO Species Adsorbed on the Au⁰ and Ti^{+δ} Sites of a 1 % Au/TiO₂ Catalyst Using In Situ FTIR Spectroscopy under Adsorption Equilibrium. *J. Am. Chem. Soc.* **2004**, *126*, 13010–13015.
- (17) Poelsema, B.; Comsa, G. *Scattering of Thermal Energy Atoms*; Springer Tracts in Modern Physics; Springer-Verlag: Berlin, 1989; vol. 115.
- (18) Farias, D.; Rieder, K. H. Atomic Beam Diffraction from Solid Surfaces. *Rep. Prog. Phys.* **1998**, *61*, 1575–1664.
- (19) Oh, J.; Kondo, T.; Hatake, D.; Nakamura, J. Elastic and Inelastic Scattering Components in the Angular Intensity Distribution of He Scattered from Graphite. *Surf. Sci.* **2009**, *603*, 895–900.
- (20) Boato, G.; Cantini, P.; Salvo, C.; Tatarek, R.; Terreni, S. Atomic Vibrations at the (0001) Graphite Surface Studied by He Atom Scattering. *Surf. Sci.* **1982**, *114*, 485–497.
- (21) Clark, G. W.; Kesmodel, L. L. Ultrahigh Vacuum Scanning Tunneling Microscopy Studies of Platinum on Graphite. *J. Vac. Sci. Technol. B* **1993**, *11*, 131–136.
- (22) Hammer, B.; Nørskov, J. K. Electronic Factors Determining the Reactivity of Metal Surfaces. *Surf. Sci.* **1995**, *343*, 211–220.
- (23) Mavrikakis, M.; Hammer, B.; Nørskov, J. K. Effect of Strain on the Reactivity of Metal Surfaces. *Phys. Rev. Lett.* **1998**, *81*, 2819–2822.
- (24) (a) Kondo, T.; Kato, H. S.; Yamada, T.; Yamamoto, S.; Kawai, M. Effect of the Molecular Structure on the Gas-Surface Scattering Studied by Supersonic Molecular Beam. *Eur. Phys. J. D* **2006**, *38*, 129–138. (b) Kondo, T.; Kato, H. S.; Bonn, M.; Kawai, M. Deposition and Crystallization Studies of Thin Amorphous Solid Water Films on Ru(0001) and on CO-Precovered Ru(0001). *J. Chem. Phys.* **2007**, *127*, 094703–094714.